Journal of Luminescence 258 (2023) 119799

Contents lists available at ScienceDirect

Journal of Luminescence

journal homepage: www.elsevier.com/locate/jlumin

Full Length Article

Surface/interface engineering of InAs quantum dot edge-emitting diodes toward III-V/SiN photonic integration

Yaonan Hou [a,*], Ilias Skandalos [a], Mingchu Tang [b,*], Hui Jia [b], Huiwen Deng [b], Xuezhe Yu [b], Yasir Noori [a], Spyros Stathopoulos [a], Siming Chen [b], Huiyun Liu [b], Alwyn Seeds [b], Graham Reed [a], Frederic Gardes [a]

[a] Optoelectronics Research Centre, University of Southampton, University Road, Southampton, SO17 1BJ, United Kingdom
[b] Department of Electronic and Electrical Engineering, University College London, Torrington Place, London, WC1E 7JE, United Kingdom

ARTICLE INFO

Keywords:
InAs
Quantum dot
Silicon nitride
Surface passivation
Photonic integration

ABSTRACT

We investigate the surface and interface engineering on InAs quantum dot (QD) emitters, by fabricating and measuring a series of edge-emitting light-emitting diodes. These diodes are encapsulated with non-stoichiometric silicon nitride (SiN) layers with various refractive indices. By analysing the optical and electrical characteristics, it is concluded that Si-rich SiN is an excellent candidate for both electrical and optical passisvations with reduced surface recombination. While the N-rich SiN deposited by the same method shows an improved device performance under optical pumping, the passivation does not appear to be as effective under electrical injection. Our findings provide important information related to the surface engineering of the interface between InAs QD stacks and non-stoichiometric SiN materials, which is arguably one of the crucial steps required to establish monolithic integration of InAs QD emitters with CMOS photonics components.

1. Introduction

Recent advances in InAs quantum dot (QD) optoelectronics grown on Si offer a potential for a substantial breakthrough in monolithic integration of III-V and Si photonics [1–3]. In particular, the achievements in electrically pumped lasers with low thresholds working at room temperature enable the fabrication of on-chip coherent light sources [4], the only missing component of a photonic integrated circuit (PIC) [5–7]. So far, various types of InAs QD lasers with high-performance have been developed, *e.g.,* QD photonic crystal lasers [8], micro-ring lasers [9], coupled-cavity tunable QD lasers [10], QD distributed-feedback lasers [11,12], and waveguide-integrated QD lasers [13,14]. Despite the fact that QDs have superior optical properties due to the high electronic density of states and the avoidance of threading dislocations during growth compared with those of quantum wells (QW) or double heterostructure (DH) configurations [15], it is imperative to passivate the surface states, which could dominate the carrier recombination and thus the emission properties of a QD photonic device [16,17]. To achieve an acceptable passivation layer, substantial efforts have been made using various materials including dielectrics based on oxides and nitrides [18,19], III-Vs [20] and even polymers [21] with *in-situ* and post-growth deposition methods. These works have mostly focused on reducing the surface recombinations of stand-alone III/V optoelectronic devices in order to improve the device performances, while omitting the influence of the refractive indices of the passivation materials. However, the refractive indices of these layers play an important role in order to enable bridging CMOS photonic circuitry and monolithically grown on-chip emitters [22].

Plasma enhanced chemical vapour deposition (PECVD) of non-stoichiometric SiN is attracting substantial interests for waveguide-based components in Si photonics due to its low optical loss, wide transparency window, non linear properties and compatibility with complementary metal-oxide semiconductors (CMOS) technology for front-end and back-end processes. Furthermore, it is possible to tune the material refractive index of the film by changing the Silicon/Nitrogen ratio [23]. This provides a possibility to passivate InAs QDs with a suitable refractive index enabling a large flexibility of designs for the monolithic integration of CMOS based photonics circuit and GaAs/SiN integrated systems.

In this work, InAs QD based edge-emitting light-emitting diodes (ELEDs) working at a wavelength of 1200-1300 nm have been selected, as this emitter structure is not only ready for fibre-optic communica-

* Corresponding authors.
E-mail addresses: yaonan.hou@soton.ac.uk (Y. Hou), mingchu.tang.11@ucl.ac.uk (M. Tang).

https://doi.org/10.1016/j.jlumin.2023.119799
Received 13 January 2023; Received in revised form 24 February 2023; Accepted 8 March 2023
Available online 15 March 2023

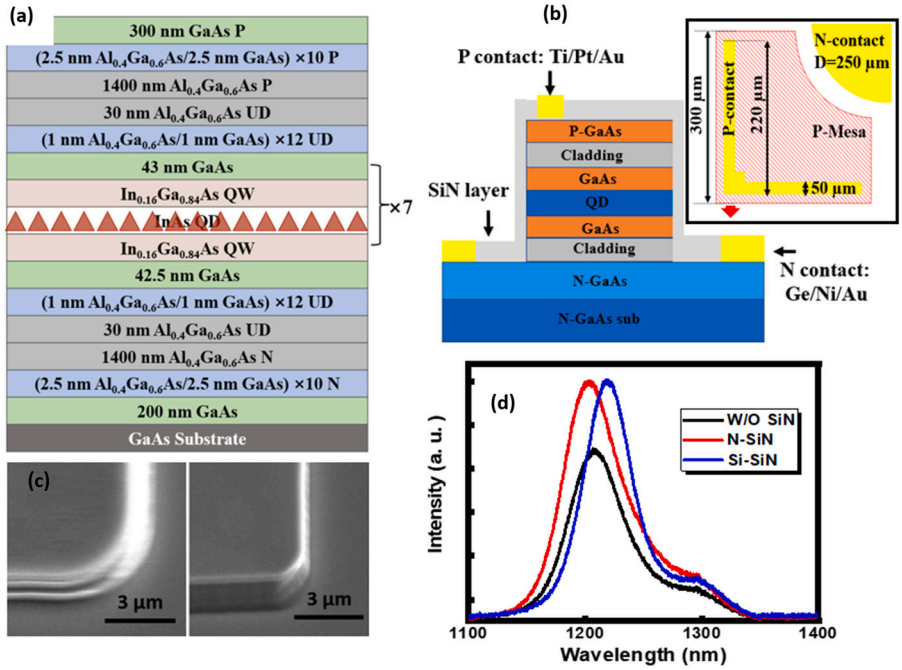

Fig. 1. (a) Epitaxial layers of the sample for ELEDs. (b) Diagram of the device structure (inset is schematic top-view of the electrodes). (c) Tilted SEM view of the mesa before (left) and after (right) chemical treatments, (d) μ-PL spectra of the ELEDs.

tions [24,25], but also similar to that of the superluminescent light-emitting diodes and the edge-emitting laser diodes [26–29], which have been achieved with InAs QDs grown on Si. The coating layers are fabricated from both Si-rich SiN (Si-SiN with refractive index $n_{Si-SiN} = 2.50 > n_{Si_3N_4} = 2.0$) and nitrogen-rich SiN (N-SiN with refractive index $n_{N-SiN} = 1.95 < n_{Si_3N_4} = 2.0$) [30]. Measurements indicate that with an SiN passivation layer both the electrical and optical characteristics of the light source can be improved (*e.g.*, EL/PL with a 1.7/1.3 enhancement factor under 130 mA/46 mW). In addition, an enhancement of the photoresponse is observed when the device is operated as a detector. The increase in performance of the device is attributed to the reduced surface recombination by passivation with Si-SiN, while the device passivated with N-SiN has a relatively lower emission intensity under electrical injection due to an excess of interface states [31].

2. Experimental methods

The InAs QD sample employed for fabricating ELEDs was grown on a GaAs substrate by molecular beam epitaxy (MBE), with a working wavelength in the O-band. The dot-in-a-well (QDwell ×7) stack was cladded in between two ~ 1.5 μm thick $Al_{0.4}Ga_{0.6}As$ layers and contact layers to form the waveguide structure (detailed information of the sample is shown in Fig. 1a). For device fabrication, the sample was firstly dry-etched down to the n-GaAs contact layer by inductively coupled plasma (ICP) to form the mesas. Subsequently, the exposed sidewalls surfaces were treated with a citric acid mixture ($C_6H_8O_7$:H_2O_2 = 20:1 for 30 sec) and ammonia (34% for 90 sec) in order to generate a smooth (to remove out-most layer destroyed by ion bombardments) and oxide-free surface (to avoid any potentially oxide-related non-radiative centres) [32,33]. Then the Si-SiN or N-SiN passivation layers with a thickness of 130/270 nm were deposited on the sidewalls/top of the structures by PECVD. Finally, metal contacts for n-type (Ge/Ni/Au) and p-type (Ti/Pt/Au) were deposited by opening vias on the n-type and p-type contact layers followed by rapid thermal annealing at 440 and 420 ^oC, respectively.

Optical properties were explored using a μ-PL system with a 785 nm excitation laser. The laser beam was focused on the sample with a ×10 objective lens (with a spot diameter of ~ 4 μm). PL collected from the same objective was sent to a spectrometer (Andor Kymera 328i) to measure the emission spectra. The electroluminescence (EL) spectra were acquired by collecting the emission from the edge of the devices using a cleaved fibre coupled to the same spectrometer, while the integrated EL intensity was measured with an InGaAs detector (Agilent 8164B, Lightwave Measurement System). The photoresponse was measured by illuminating the device from the top with a fibre-coupled laser with wavelength tuned from 1260 to 1360 nm (Agilent 8164B, Lightwave Measurement System). The external bias and measured current were recorded with a source-metre unit (Keithley 2401 SMU) at 0 V bias. All the electrical and optical tests were conducted at room temperature.

3. Results

Three ELEDs were fabricated in total: two of them encapsulated with Si-SiN (n = 2.50) and N-SiN (n = 1.95); and another without surface passivisation as a control device (detailed information of the epitaxial wafer and schematic of the cross-sectional device structure are shown in Fig. 1a Fig. 1b, respectively). Scanning electron microscope (SEM) measurements reveal that the effective sidewall smoothing process due to wet treatment (Fig. 1c) [34]. Owing to the directivity of the plasma enhanced deposition method, the deposited thicknesses of SiN on the top and sidewall of the ELEDs are 270 nm and 130 nm respectively [28]. Same thickness are deposited is to study the surface passivation with different stoichiometry and not to optimize the emission intensity in our work. The inset of Fig. 1b shows dimensions and shapes of the electrodes as well as the mesa of our ELEDs.

Fig. 1d displays the room-temperature μ-PL spectra of the three ELEDs under pumping power intensity of 372 kW/cm^2. A clear main peak at ~ 1200 nm with a shoulder at ~ 1300 nm can be observed, attributed to the excited and ground state recombination respectively. The dominant emission at the excited state is due to the high excitation power intensity, confirmed by comparing with the PL with low excitation power density (not to show) [35]. The slight difference between the emission peaks is likely the result of different strain introduced by the coating layer with different stoichiometry [36–38], which further affects the energy band structure and carrier transitions [39].

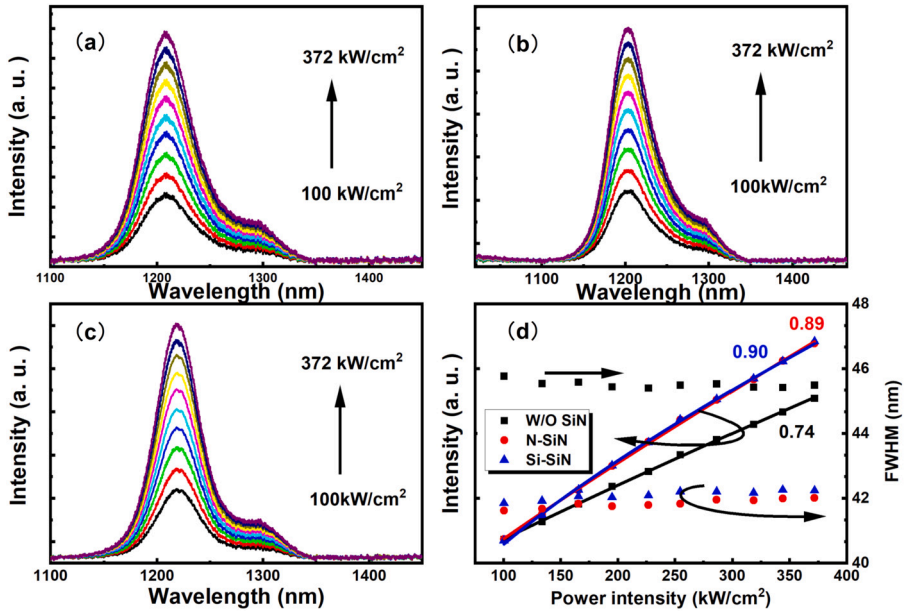

Fig. 2. Power-dependent μ-PL measurements of ELEDs without coating (a) with Si-SiN coating (b) and with N-SiN coating (c), and (d) Intensity and FWHM as a function of pumping power.

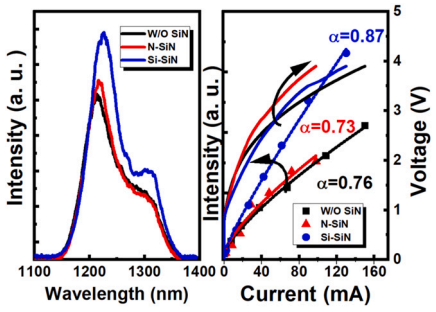

Fig. 3. (a) EL spectra of the ELEDs under 100 mA. (b) L-I-V of the diodes.

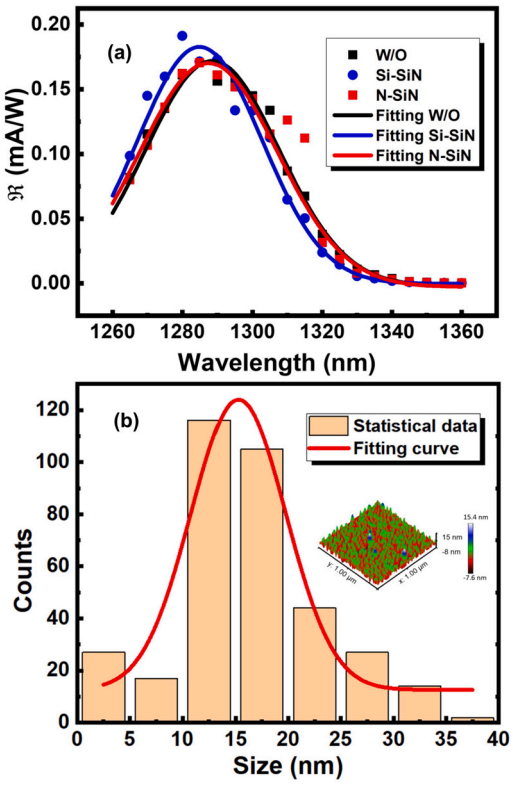

Fig. 4. (a) Spectral photoresponse of the diodes, (b) Lateral size distribution measured from AFM (inset).

Power-dependent PL measurements are shown in Figs. 2a-c. All the PL spectra exhibit a main emission peak at ~ 1200 nm as discussed. Fig. 2d shows the panchromatic integrated PL intensity as a function of the pumping power intensity. The relationship can be fitted into the power function, $I \propto I_0^{\alpha}$, where I_0 is the excitation power intensity and α the exponent. Ideally, a linear curve ($\alpha = 1$) can be expected for direct band gap materials supposing there is no non-radiative recombination. While the curve degrades to sub-linear style ($\alpha < 1$) once the non-radiative recombination exists [40]. In this work, all the devices are fabricated from identical wafers with three different surface coatings, where the differences in the fitting curves can only be attributed to the results of the surface-related recombinations. From the fitting we observed that the exponent of the devices with Si-SiN, N-SiN and without coating are 0.90, 0.89 and 0.74 (as shown in Fig. 2d), indicating that non-stoichiometric SiN indeed works well as surface passivation layer in improving the optical properties of InAs QDs. In addition, it is also observable that the linewidth of the non-passivated device is 46 nm, which further decreases to 42 nm for the passivated devices due to reduced "spectral diffusion" caused by the surface defects [41,42].

The device properties under electrical injection was investigated by measuring the EL under increasing biased currents up to 100 mA from the facet. Before this, we coarsely scanned the emission around the edges of the device. The strongest emission was found and recorded underneath the electrodes (inset of Fig. 1b). Fig. 3a shows the emission spectrum of the three ELEDs under 100 mA. The spectra possess a shape equivalent to the PLs, whilst a slight redshift of the peaks is attributed to the band gap shrinkage due to the high injected carrier density. The average linewidth of the main peak increases from 44 to 50 nm with current increasing from 10 to 100 mA, ascribed to the holes thermally broadened by their closely spaced energy levels [43]. Fig. 4d illustrates the measured light-current-voltage (L-I-V) curves of the ELEDs (intensity is panchromatic integrated value). All devices exhibit a turn-on voltage at ~ 1 V which agrees with edge-emitting diodes fabricated with similar epitaxial layers [44], indicating the normal operation of the fabricated devices. Similar to the case of power-dependent PL, the curve

can be fitted into power function in order to study the carrier dynamics of the ELEDs. The fitting exponents (α) for the devices with Si-SiN, N-SiN and without coatings are 0.87, 0.73 and 0.76, respectively (Fig. 3b). It can be seen that the α values measured under electrical injection are overall lower than those under optical pumping due to the injected carriers not fully recombining at the QDs. Furthermore, under the same injection current, Si-SiN passivated ELED also exhibits higher EL intensity, which cannot be solely be attributed to the enhanced extraction efficiency considering the non-linear relationship between emission intensity and the injection current. It is also observable that the N-SiN passivated ELED is exhibiting a much lower α compared with that of the Si-SiN coated one. The reason lies at the interfaces states between the optical active layer and passivation layer. In the Si-SiN material, the Si dangling bonds, observed in previous work [45], can form stable electronic states with freshly treated III-V surfaces [46]. In contrast, the N-SiN has a much higher density of N-H bonds according to our previous study [30], which is associated with high interface state densities [31]. Therefore, additional electron overflow and non-radiative recombination might occur through such states at the N-SiN/InAs QD interfaces.

4. Discussion

Although our device is not designed for photodetectors with a high quantum efficiency, investigating photoresponse will be helpful to further understand the surface passivation to the InAs QDs. To do this, we carried out the optical response characterizations of the diode with a tunable laser from 1260 to 1360 nm. The coherence excitation ensures us to study the pure electron-hole generation and transport behaviours in the QD layers. The photocurrent was recorded at 0 V to avoid any potential issues such as current gain under a bias. Fig. 4a shows the spectral photoresponsivity of the devices. The peak positions at ~1280-1290 nm are due to the light absorption at the ground state. Given the refractive indices and thickness of the top coatings, the reflections of the incoming beam at the surface of the diode is calculated to be 29.7% (Si-SiN), 22.4% (N-SiN) and 30% (without coating), respectively. The corresponding internal quantum efficiencies (IQE) at the peak wavelengths are calculated to be 0.025%, 0.021% and 0.023%. It can be extracted from 4a that Si-SiN coated diode has the highest IQE, which again illustrates that Si-SiN is optimum for passivation of III-V/dielectric interfaces.

In addition, we observed that the photoresponse spectra are Gaussian functions with linewidth of ~46 nm (Fig. 4b), similar to that of PL/EL spectra. It is known that the emission spectrum from a semiconductor QD is Lorentzian shape according to previous work [47]. However, it could be degraded into a Gaussian shape by interacting with inhomogeneous broadening. In this case, the shape of the optical spectra is contributed to by different dimensions of InAs QDs. Fig. 4b shows the size distribution of the QDs size also fitting a Gaussian function, which has been proven to translate to optical spectrum broadening [48]. In this work, no additional optical peak and spectral broadening are introduced from both emission and absorption spectra, suggesting non-stoichiometric SiN a good passivations layer for InAs QDs.

5. Summary

In summary, we fabricated InAs QD based ELEDs fully covered with PECVD non-stoichiometric SiN coatings. The coating layers were deposited with designated refractive index and thickness. The optical and electrical characteristics were measured to study the effects of surface passivation. Our results reveal that Si-SiN is able to improve both electrical and optical properties of the ELEDs. In contrast, the diodes passivated with N-SiN exhibit enhanced emission under optical pumping, but are less effective for electrical injection due to the high density of N-H bonds, leading to potential current overflow and non-radiative recombination. Except for the enhanced optical properties, no extra defect-related emission peaks and spectra broadening were observed by introducing SiN passivations. Overall, our work offers a possibility to engineer the interface between III-V gains and non-stoichiometric SiN passives for Si photonic integration.

CRediT authorship contribution statement

Conception and design of study: Y. Hou, F. Gardes, A. Seeds, G. Reed, H. Liu.

Material growth: M. Tang, H. Jia, H. Deng, X. Yu, S. Chen, H. Liu.

Device fabrication: Y. Hou, S. Stathopoulos, Y. Noori.

Device test: Y. Hou, I. Skandalos.

Manuscript preparation: Y. Hou, F. Gardes, A. Seeds, G. Reed, H. Liu, I. Skandalos, M. Tang, H. Jia, H. Deng. S. Chen, S. Stathopoulos, Y. Noori, X. Yu.

Declaration of competing interest

The authors declare that they have no known competing financial interests or personal relationships that could have appeared to influence the work reported in this paper.

Data availability

Data will be made available on request.

Acknowledgements

The authors are grateful for support from the UKRI-EPSRC Programme Grant “QUantum Dot On Silicon systems for communications, information processing and sensing (QUDOS)” under the grant number of EP/T028475/1. For the purpose of open access, the author has applied a Creative Commons Attribution* (CCBY) licence to any Author Accepted Manuscript version arising.

References

[1] M. Tang, J.-S. Park, Z. Wang, S. Chen, P. Jurczak, A. Seeds, H. Liu, Integration of iii-v lasers on si for si photonics, Prog. Quantum Electron. 66 (2019) 1–18.

[2] C. Shang, Y. Wan, J. Selvidge, E. Hughes, R. Herrick, K. Mukherjee, J. Duan, F. Grillot, W.W. Chow, J.E. Bowers, Perspectives on advances in quantum dot lasers and integration with si photonic integrated circuits, ACS Photonics 8 (9) (2021) 2555–2566.

[3] K. Nishi, K. Takemasa, M. Sugawara, Y. Arakawa, Development of quantum dot lasers for data-com and silicon photonics applications, IEEE J. Sel. Top. Quantum Electron. 23 (6) (2017) 1–7.

[4] S. Chen, W. Li, J. Wu, Q. Jiang, M. Tang, S. Shutts, S.N. Elliott, A. Sobiesierski, A.J. Seeds, I. Ross, et al., Electrically pumped continuous-wave iii–v quantum dot lasers on silicon, Nat. Photonics 10 (5) (2016) 307–311.

[5] E. Marchena, T. Creazzo, S.B. Krasulick, K. Paul, D. Van Orden, J.Y. Spann, C.C. Blivin, J.M. Dallesasse, P. Varangis, R.J. Stone, et al., Integrated tunable cmos laser for si photonics, in: 2013 Optical Fiber Communication Conference and Exposition and the National Fiber Optic Engineers Conference (OFC/NFOEC), IEEE, 2013, pp. 1–3.

[6] Y. Shi, B. Kunert, Y. De Koninck, M. Pantouvaki, J. Van Campenhout, D. Van Thourhout, Novel adiabatic coupler for iii-v nano-ridge laser grown on a si photonics platform, Opt. Express 27 (26) (2019) 37781–37794.

[7] A. Le Liepvre, C. Jany, A. Accard, M. Lamponi, F. Poingt, D. Make, F. Lelarge, J.-M. Fedeli, S. Messaoudene, D. Bordel, et al., Widely wavelength tunable hybrid iii–v/silicon laser with 45 nm tuning range fabricated using a wafer bonding technique, in: The 9th International Conference on Group IV Photonics (GFP), IEEE, 2012, pp. 54–56.

[8] T. Zhou, M. Tang, G. Xiang, B. Xiang, S. Hark, M. Martin, T. Baron, S. Pan, J.-S. Park, Z. Liu, et al., Continuous-wave quantum dot photonic crystal lasers grown on on-axis si (001), Nat. Commun. 11 (1) (2020) 1–7.

[9] Y. Wan, J. Norman, Q. Li, M. Kennedy, D. Liang, C. Zhang, D. Huang, Z. Zhang, A.Y. Liu, A. Torres, et al., 1.3 μm submilliamp threshold quantum dot micro-lasers on si, Optica 4 (8) (2017) 940–944.

[10] Y. Wan, S. Zhang, J.C. Norman, M. Kennedy, W. He, S. Liu, C. Xiang, C. Shang, J.-J. He, A.C. Gossard, et al., Tunable quantum dot lasers grown directly on silicon, Optica 6 (11) (2019) 1394–1400.

[11] Y. Wang, S. Chen, Y. Yu, L. Zhou, L. Liu, C. Yang, M. Liao, M. Tang, Z. Liu, J. Wu, et al., Monolithic quantum-dot distributed feedback laser array on silicon, Optica 5 (5) (2018) 528–533.
[12] Y. Wan, J.C. Norman, Y. Tong, M. Kennedy, W. He, J. Selvidge, C. Shang, M. Dumont, A. Malik, H.K. Tsang, et al., 1.3 μm quantum dot-distributed feedback lasers directly grown on (001) si, Laser Photonics Rev. 14 (7) (2020) 2000037.
[13] C. Shang, K. Feng, E.T. Hughes, A. Clark, M. Debnath, R. Koscica, G. Leake, J. Herman, D. Harame, P. Ludewig, et al., Electrically pumped quantum-dot lasers grown on 300 mm patterned si photonic wafers, arXiv preprint arXiv:2206.01211, 2022.
[14] Y. Wan, C. Xiang, J. Guo, R. Koscica, M. Kennedy, J. Selvidge, Z. Zhang, L. Chang, W. Xie, D. Huang, et al., High speed evanescent quantum-dot lasers on si, Laser Photonics Rev. 15 (8) (2021) 2100057.
[15] Z. Liu, C. Hantschmann, M. Tang, Y. Lu, J.-S. Park, M. Liao, S. Pan, A. Sanchez, R. Beanland, M. Martin, et al., Origin of defect tolerance in inas/gaas quantum dot lasers grown on silicon, J. Lightwave Technol. 38 (2) (2019) 240–248.
[16] J. Liu, K. Konthasinghe, M. Davanço, J. Lawall, V. Anant, V. Verma, R. Mirin, S.W. Nam, J.D. Song, B. Ma, et al., Single self-assembled inas/gaas quantum dots in photonic nanostructures: the role of nanofabrication, Phys. Rev. Appl. 9 (6) (2018) 064019.
[17] H.J. Song, C.H. Roh, J.H. Lee, H.G. Choi, D.H. Kim, J.H. Park, C.-K. Hahn, Analysis of surface dark current dependent upon surface passivation in apd based on gaas, Semicond. Sci. Technol. 24 (6) (2009) 065003.
[18] S. Manna, H. Huang, S.F.C. da Silva, C. Schimpf, M.B. Rota, B. Lehner, M. Reindl, R. Trotta, A. Rastelli, Surface passivation and oxide encapsulation to improve optical properties of a single gaas quantum dot close to the surface, Appl. Surf. Sci. 532 (2020) 147360.
[19] A. Chellu, E. Koivusalo, M. Raappana, S. Ranta, V. Polojärvi, A. Tukiainen, K. Lahtonen, J. Saari, M. Valden, H. Seppänen, et al., Gaas surface passivation for inas/gaas quantum dot based nanophotonic devices, Nanotechnology 32 (13) (2021) 130001.
[20] P. Jurczak, Y. Zhang, J. Wu, A.M. Sanchez, M. Aagesen, H. Liu, Ten-fold enhancement of inas nanowire photoluminescence emission with an inp passivation layer, Nano Lett. 17 (6) (2017) 3629–3633.
[21] H.J. Song, C.H. Roh, J.H. Lee, H.G. Choi, D.H. Kim, J.H. Park, C.-K. Hahn, Comparative analysis of dark current between sinx and polyimide surface passivation of an avalanche photodiode based on gaas, Semicond. Sci. Technol. 24 (5) (2009) 055012.
[22] H. Park, Integrated active devices with improved optical coupling to dielectric waveguides, uS Patent 10,718,898, Jul. 21 2020.
[23] F. Gardes, A. Shooa, G. De Paoli, I. Skandalos, S. Ilie, T. Rutirawut, W. Talataisong, J. Faneca, V. Vitali, Y. Hou, et al., A review of capabilities and scope for hybrid integration offered by silicon-nitride-based photonic integrated circuits, Sensors 22 (11) (2022) 4227.
[24] D. Fye, Low-current 1.3-μm edge-emitting led for single-mode fiber subscriber loop applications, J. Lightwave Technol. 4 (10) (1986) 1546–1551.
[25] H. Kressel, M. Ettenberg, A new edge-emitting (alga) as heterojunction led for fiber-optic communications, Proc. IEEE 63 (9) (1975) 1360–1361.
[26] Y. Lu, V. Cao, M. Liao, W. Li, M. Tang, A. Li, P. Smowton, A. Seeds, H. Liu, S. Chen, Electrically pumped continuous-wave o-band quantum-dot superluminescent diode on silicon, Opt. Lett. 45 (19) (2020) 5468–5471.
[27] S. Chen, M. Tang, Q. Jiang, J. Wu, V.G. Dorogan, M. Benamara, Y.I. Mazur, G.J. Salamo, P. Smowton, A. Seeds, et al., Inas/gaas quantum-dot superluminescent light-emitting diode monolithically grown on a si substrate, ACS Photonics 1 (7) (2014) 638–642.
[28] M. Tang, S. Chen, J. Wu, Q. Jiang, K. Kennedy, P. Jurczak, M. Liao, R. Beanland, A. Seeds, H. Liu, Optimizations of defect filter layers for 1.3-μm inas/gaas quantum-dot lasers monolithically grown on si substrates, IEEE J. Sel. Top. Quantum Electron. 22 (6) (2016) 50–56.
[29] S. Chen, M. Tang, J. Wu, Q. Jiang, V. Dorogan, M. Benamara, Y. Mazur, G. Salamo, A.J. Seeds, H. Liu, 1.3 μm inas/gaas quantum-dot laser monolithically grown on si substrates operating over 100° c, Electron. Lett. 50 (20) (2014) 1467–1468.
[30] T.D. Bucio, C. Lacava, M. Clementi, J. Faneca, I. Skandalos, A. Baldycheva, M. Galli, K. Debnath, P. Petropoulos, F. Gardes, Silicon nitride photonics for the near-infrared, IEEE J. Sel. Top. Quantum Electron. 26 (2) (2019) 1–13.
[31] S. Pal, D. Bose, Fabrication and characterization of gaas mis devices with n-rich pecvd sixny dielectric, Appl. Surf. Sci. 181 (3–4) (2001) 179–184.
[32] T. Baum, S. Ye, K. Uosaki, Formation of self-assembled monolayers of alkanethiols on gaas surface with in situ surface activation by ammonium hydroxide, Langmuir 15 (25) (1999) 8577–8579.
[33] W.J. Fritz, L.B. Bauer, C.S. Miller, Analysis of aluminum gallium arsenide laser diodes failing due to nonradiative regions behind the facets, in: 27th Annual Proceedings, International Reliability Physics Symposium, IEEE, 1989, pp. 59–64.
[34] C. Juang, K. Kuhn, R. Darling, Selective etching of gaas and al0. 30ga0. 70as with citric acid/hydrogen peroxide solutions, J. Vac. Sci. Technol., B Microelectron. Process. Phenom. 8 (5) (1990) 1122–1124.
[35] H. Djie, B. Ooi, X.-M. Fang, Y. Wu, J. Fastenau, W. Liu, M. Hopkinson, Room-temperature broadband emission of an ingaas/gaas quantum dots laser, Opt. Lett. 32 (1) (2007) 44–46.
[36] C. Blaauw, Stress in chemical-vapor-deposited sio2 and plasma-sin x films on gaas and si, J. Appl. Phys. 54 (9) (1983) 5064–5068.
[37] V. Au, C. Charles, D. Bulla, J. Love, R. Boswell, Thickness-dependent stress in plasma-deposited silicon dioxide films, J. Appl. Phys. 97 (8) (2005) 084912.
[38] K. Mackenzie, D. Johnson, M. DeVre, R. Westerman, B. Reelfs, Stress control of si-based pecvd dielectrics, in: Proceedings of the 207th Electrochemical Society Meeting, 2005, pp. 148–159.
[39] K. Omambac, J. Porquez, J. Afalla, D. Vasquez, M. Balgos, R. Jaculbia, A. Somintac, A. Salvador, Application of external tensile and compressive strain on a single layer InAs/GaAs quantum dot via epitaxial lift-off, Phys. Status Solidi B 250 (8) (2013) 1632–1635.
[40] V. Fedorenko, R. Viter, R. Mrówczyński, D. Damberga, E. Coy, I. Iatsunskyi, Synthesis and photoluminescence properties of hybrid 1d core–shell structured nanocomposites based on zno/polydopamine, RSC Adv. 10 (50) (2020) 29751–29758.
[41] M. Abbarchi, F. Troiani, C. Mastrandrea, G. Goldoni, T. Kuroda, T. Mano, K. Sakoda, N. Koguchi, S. Sanguinetti, A. Vinattieri, et al., Spectral diffusion and line broadening in single self-assembled ga as/ al ga as quantum dot photoluminescence, Appl. Phys. Lett. 93 (16) (2008) 162101.
[42] N. Ha, T. Mano, Y.-L. Chou, Y.-N. Wu, S.-J. Cheng, J. Bocquel, P.M. Koenraad, A. Ohtake, Y. Sakuma, K. Sakoda, et al., Size-dependent line broadening in the emission spectra of single gaas quantum dots: impact of surface charge on spectral diffusion, Phys. Rev. B 92 (7) (2015) 075306.
[43] O.á. Shchekin, D. Deppe, 1.3 μm inas quantum dot laser with t o= 161 k from 0 to 80 c, Appl. Phys. Lett. 80 (18) (2002) 3277–3279.
[44] K. Li, Z. Liu, M. Tang, M. Liao, D. Kim, H. Deng, A.M. Sanchez, R. Beanland, M. Martin, T. Baron, et al., O-band inas/gaas quantum dot laser monolithically integrated on exact (0 0 1) si substrate, J. Cryst. Growth 511 (2019) 56–60.
[45] W. Lau, S. Fonash, J. Kanicki, Stability of electrical properties of nitrogen-rich, silicon-rich, and stoichiometric silicon nitride films, J. Appl. Phys. 66 (6) (1989) 2765–2767.
[46] S. Oktyabrsky, V. Tokranov, M. Yakimov, R. Moore, S. Koveshnikov, W. Tsai, F. Zhu, J. Lee, High-k gate stack on gaas and ingaas using in situ passivation with amorphous silicon, Mater. Sci. Eng. B 135 (3) (2006) 272–276.
[47] P. Lodahl, S. Mahmoodian, S. Stobbe, Interfacing single photons and single quantum dots with photonic nanostructures, Rev. Mod. Phys. 87 (2) (2015) 347.
[48] R.M. Makhijani, S. Chakrabarti, V.A. Singh, Photoluminescence spectra of inas quantum dots embedded in gaas heterostructure, J. Lumin. 136 (2013) 401–406.